The Plant Cell, Vol. 22: 797–810, March 2010, www.plantcell.org

Internal Architecture of Mitochondrial Complex I from *Arabidopsis thaliana*

Jennifer Klodmann,[a] Stephanie Sunderhaus,[a] Manfred Nimtz,[b] Lothar Jänsch,[b] and Hans-Peter Braun[a,1]

[a] Institute for Plant Genetics, Faculty of Natural Sciences, Leibniz Universität Hannover, D-30419 Hannover, Germany
[b] Proteome Research Group, Division of Cell and Immune Biology, Helmholtz Centre for Infection Research, D-38124 Braunschweig, Germany

The NADH dehydrogenase complex (complex I) of the respiratory chain has unique features in plants. It is the main entrance site for electrons into the respiratory electron transfer chain, has a role in maintaining the redox balance of the entire plant cell and additionally comprises enzymatic side activities essential for other metabolic pathways. Here, we present a proteomic investigation to elucidate its internal structure. *Arabidopsis thaliana* complex I was purified by a gentle biochemical procedure that includes a cytochrome c–mediated depletion of other respiratory protein complexes. To examine its internal subunit arrangement, isolated complex I was dissected into subcomplexes. Controlled disassembly of the holo complex (1000 kD) by low-concentration SDS treatment produced 10 subcomplexes of 550, 450, 370, 270, 240, 210, 160, 140, 140, and 85 kD. Systematic analyses of subunit composition by mass spectrometry gave insights into subunit arrangement within complex I. Overall, *Arabidopsis* complex I includes at least 49 subunits, 17 of which are unique to plants. Subunits form subcomplexes analogous to the known functional modules of complex I from heterotrophic eukaryotes (the so-called N-, Q-, and P-modules), but also additional modules, most notably an 85-kD domain including γ-type carbonic anhydrases. Based on topological information for many of its subunits, we present a model of the internal architecture of plant complex I.

INTRODUCTION

Oxidative phosphorylation (OXPHOS) is the ATP formation driven by oxidative reactions of the respiratory chain. The process is based on the presence of a so-called OXPHOS system localized in specialized biomembranes (e.g., the plasma membrane in oxygenic prokaryotes and the inner mitochondrial membrane in eukaryotes). Complex I is the largest protein complex of the OXPHOS system (for reviews, see Friedrich and Böttcher, 2004; Brandt, 2006; Vogel et al., 2007; Remacle et al., 2008; Zickermann et al., 2008, 2009; Lazarou et al., 2009). It catalyzes NADH-quinone oxidoreduction and in many systems represents the main entrance site for electrons into the respiratory electron transfer chain. Coupled to this oxidoreduction, complex I translocates protons across the inner mitochondrial membrane or the plasma membrane of bacteria. The precise mechanism of complex I function is still not completely understood (reviewed in Zickermann et al., 2009).

Analyses by electron microscopy (EM) revealed that complex I is composed of two arms arranged in orthogonal configuration to form an L-shaped particle (Guénebaut et al., 1997, 1998; Grigorieff, 1998; Böttcher et al., 2002; Peng et al., 2003; Dudkina et al., 2005; Radermacher et al., 2006; Morgan and Sazanov, 2008; Clason et al., 2010). One arm is hydrophobic and embedded within the membrane (membrane arm); the other is hydrophilic and protrudes into the mitochondrial matrix or the lumen of a bacterial cell (peripheral arm). In *Escherichia coli*, complex I is composed of 14 subunits but in mitochondria complex I contains up to 31 additional subunits. The structure of the peripheral arm of the archaebacterium *Thermus thermophilus* complex I was recently solved by x-ray crystallography. It includes eight subunits that bind one flavine mononucleotide and nine iron-sulfur clusters as redox prosthetic groups involved in electron transfer from NADH to quinone (Hinchliffe and Sazanov, 2005; Sazanov and Hinchliffe, 2006; Sazanov, 2007; Berrisford and Sazanov, 2009). By contrast, the inner architecture of the membrane arm, which is responsible for proton translocation, is less well understood. Locations of some subunits have been deduced by single particle electron microscopy using complex I subcomplexes or by immune-electron microscopy (Abdrakhmanova et al., 2004; Baranova et al., 2007a, 2007b; Clason et al., 2007). Overall, the subunits of the prokaryotic membrane arm are predicted to include >50 membrane-spanning helices. Even more membrane-spanning helices are predicted to be present within the membrane arm of eukaryotic complex I. Seven of the most hydrophobic subunits of the membrane arm in eukaryotes are encoded by the mitochondrial genome in most organisms investigated.

Nomenclature of complex I subunits unfortunately differs among the organisms investigated, although a large number of subunits likewise are present in different species. In this work,

[1] Address correspondence to braun@genetik.uni-hannover.de.
The author responsible for distribution of materials integral to the findings presented in this article in accordance with the policy described in the Instructions for Authors (www.plantcell.org) is: Hans-Peter Braun (braun@genetik.uni-hannover.de).
www.plantcell.org/cgi/doi/10.1105/tpc.109.073726

the bovine nomenclature is used for all homologous complex I subunits of Arabidopsis because bovine complex I is particularly well-investigated (Carroll et al., 2003, 2006; Hirst et al., 2003). Subunits specific to complex I of plant mitochondria are named according to the corresponding genes annotated by The Arabidopsis Information Resource (TAIR; www.Arabidopsis.org).

The OXPHOS system of plant mitochondria is more complicated compared with its counterparts in heterotrophic eukaryotes. First of all, quite a large number of alternative oxidoreductases are present in the inner mitochondrial membrane; these participate in respiratory electron transport without contributing to the proton gradient across the inner mitochondrial membrane (reviewed in Rasmusson et al., 2008). Furthermore, the classical protein complexes of the OXPHOS system have several special features. Complex I of *Arabidopsis*, rice (*Oryza sativa*), and *Chlamydomonas reinhardtii* was reported to include plant-specific subunits (Heazlewood et al., 2003; Millar et al., 2003; Cardol et al., 2004; Sunderhaus et al., 2006; Meyer et al., 2008). So far, 13 complex I subunits of *Arabidopsis* that have no counterparts in complex I of mammals or fungi have been described. Some of these subunits introduce side activities into complex I, for example, subunits resembling γ-type carbonic anhydrases (CAs) and an L-galactone-1,4-lactone dehydrogenase (GLDH), which is associated with complex I in plants.

In plants, mitochondrial complex I has additional functions that are of great importance for the entire cell, e.g., in maintaining the redox balance during photosynthesis (Dutilleul et al., 2003). Also, plant complex I has a unique shape as revealed by single-particle EM (Dudkina et al., 2005; Sunderhaus et al., 2006; Peters et al., 2008; Bultema et al., 2009). In contrast with all other investigated organisms, it comprises an additional peripheral domain that is attached to the membrane arm at a central position on its matrix-exposed side (Figure 1). The extra domain has a spherical shape, is estimated to have a molecular mass of 80 kD, and was shown to include CA subunits specific for plant complex I (Sunderhaus et al., 2006). By analogy with the prototype CA from the archaebacterium *Methanosarcina thermophila* (CAM) (Alber and Ferry, 1994), the spherical extra domain probably represents a CA trimer. Three distinct CAs have been found to be present within *Arabidopsis* complex I and are termed CA1, CA2, and CA3. Furthermore, two CA-like proteins named CAL1 and CAL2 have been described that have altered active sites compared with the one of CAM (reviewed in Braun and Zabaleta, 2007). The physiological role of the CA domain of plant complex I is currently a matter of debate.

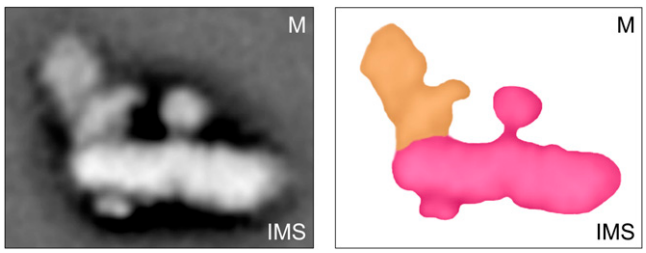

Figure 1. EM Average Structure and Scheme of Mitochondrial Complex I from *Arabidopsis*.

The EM average structure (left) was taken from Dudkina et al. (2005). The deduced scheme (right) shows the membrane arm of complex I in red and the peripheral arm in orange. The membrane arm is inserted into the inner mitochondrial membrane. M, matrix side; IMS, intermembrane space side.

To better understand structure and function of plant complex I, we analyzed its internal architecture. The study is based on a biochemical strategy that includes gentle complex I purification, controlled disassembly of the purified complex, separation of the generated subcomplexes by blue native (BN)-PAGE, separation of the subunits of the subcomplexes by SDS-PAGE, and, finally, subunit identification by tandem mass spectrometry. Integration of the obtained results is used to deduce the internal architecture of plant complex I.

RESULTS

Purification of Complex I from *Arabidopsis*

Biochemical analysis of the subunit arrangement within complex I first requires its gentle purification in the native conformation. A new three-step purification strategy was developed for complex I isolation, based on (1) purification of mitochondrial membranes, (2) separation of mitochondrial membrane protein complexes by sucrose gradient ultracentrifugation, and, finally, (3) cytochrome c affinity chromatography to remove complex III and complex III–containing supercomplexes from complex I–enriched fractions (Figure 2). The outcome of each purification step can be monitored by one-dimensional (1D) BN-PAGE.

The starting point for the complex I purification was mitochondria isolated from *Arabidopsis* cell suspension cultures. The organelle fraction included all five OXPHOS complexes, the I+III_2 supercomplex and the F1 part of complex V (Figure 2A). Since complex I is the largest enzyme of the OXPHOS system, a size-based separation by sucrose gradient ultracentrifugation was employed to separate the solubilized complexes of the mitochondrial membranes. Under the conditions applied, complex I–enriched fractions were located close the bottom of the centrifugation tube (Figure 2B, fractions 2 and 3). The only visible contaminations within theses fractions were dimeric complex III and the I+III_2 supercomplex.

Finally, cytochrome c affinity chromatography was applied to specifically remove complex III_2 and the I+III_2 supercomplex from complex I–enriched fractions. Originally, this procedure was developed to purify complex III_2 by the binding to its natural substrate cytochrome c (Weiss and Juchs, 1978; Braun and Schmitz, 1992). Binding of complex III_2 is most efficient if cytochrome c is in the oxidized state. Upon reduction of cytochrome c by ascorbate, affinity decreases and allows elution of complex III by a salt gradient of low ionic strength (Weiss and Juchs, 1978). No salt gradient is necessary to detach complex I from the cytochrome c sepharose because it simply passes through the column without interactions and therefore can be obtained in the flow-through fraction. Low salt conditions during purification ensure optimal integrity and native conformation of complex I (Figure 2C).

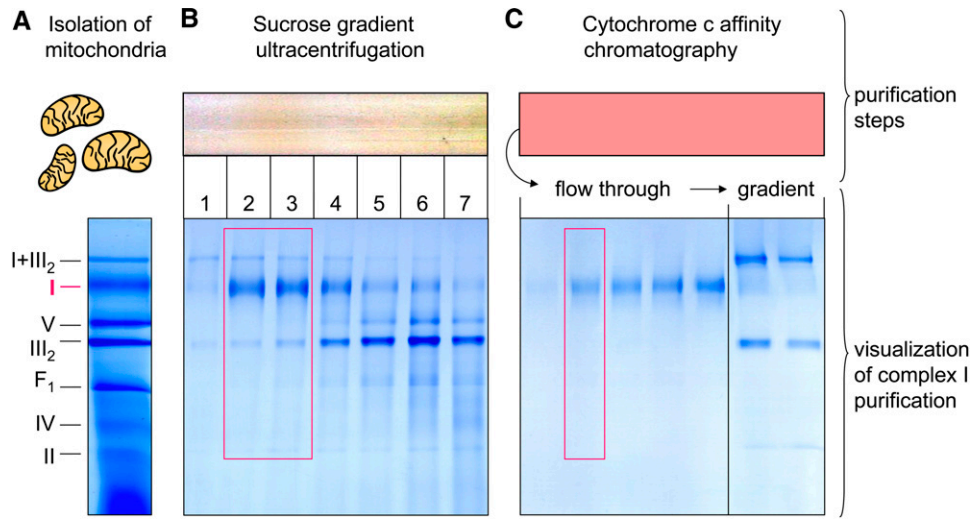

Figure 2. Purification Strategy for Mitochondrial Complex I of *Arabidopsis*.

The three purification steps are shown at the top; after each step, complex I purity was visualized by BN-PAGE and Coomassie blue staining.
(A) Mitochondria were isolated from *Arabidopsis* suspension culture, and total membrane protein was extracted. All OXPHOS complexes are present within this fraction as monitored by BN-PAGE (gel below). Identification of bands was based on subunit composition of the complexes as revealed by second gel dimensions (for comparison, see Eubel et al., 2003). I, II, IV, and V, complexes I, II, IV, and V; F_1, F1 part of complex V; III_2, dimeric complex III; $I+III_2$, supercomplex composed of complex I and dimeric complex III.
(B) The membrane proteins were subsequently separated by sucrose gradient ultracentrifugation. The top of the gradient (small protein complexes) is to the right and the bottom (large protein complexes) to the left. Complex I-containing fractions were identified by BN-PAGE (gel below, rectangle).
(C) These fractions were used for cytochrome c affinity chromatography. Complex I was obtained in the flow-through as revealed by BN-PAGE (gel below, rectangle). Finally, complex III_2 and the $I+III_2$ supercomplex were eluted from the column with a salt gradient as visible on the BN gel shown below.

Controlled Disassembly of *Arabidopsis* Complex I

To obtain information on subunit localizations within complex I, the isolated protein complex was destabilized using defined biochemical conditions to generate complex I subcomplexes and finally analyze their subunit composition. Several destabilization conditions were tested, such as temperature, urea, and detergent treatment or mild proteolysis. Results of experiments were monitored by 1D BN-PAGE. Many conditions allowed dissecting complex I (1000 kD) into a large membrane arm of 550 kD and a 370-kD subcomplex that represents the peripheral arm. Dissection of isolated complex I from *Arabidopsis* into subcomplexes of similar sizes was previously reported by the use of two-dimensional (2D) BN/BN-PAGE, if digitonin used for solubilization is replaced by dodecylmaltoside during the electrophoresis run of the second native gel dimension (Sunderhaus et al., 2006). However, slightly harsher conditions than these destabilization treatments consistently caused complete disassembly of complex I into its subunits.

We finally tested destabilization of isolated complex I by treatment with SDS at very low concentrations. Indeed, several additional complex I subcomplexes became visible upon analysis by 1D BN-PAGE and subsequent Coomassie blue or NADH activity staining (Figure 3). Treatment of complex I with only 0.01% SDS caused its partial dissociation into the 550- and 370-kD subcomplexes. Also, the molecular mass of the holocomplex is slightly reduced by ~80 kD in the presence of 0.01% SDS, indicating loss of a few individual subunits (Figure 3). Increase of the SDS concentration to 0.04% and up to 0.12% generates further subcomplexes of 240, 210, and 140 kD, all of which can oxidize NADH as monitored by an in-gel activity assay. Therefore, they were considered to represent subcomplexes of the peripheral arm, which is known to include the NADH oxidation domain of complex I.

2D BN/SDS-PAGE analyses were performed to further examine SDS-induced subcomplex generation (Figure 4). In the absence of SDS, the subunits of the complex I holoenzyme form a vertical row of spots in the 1000-kD gel region (Figure 4, left gel). Treatment of intact complex I with 0.015% SDS leads to its partial dissection into the 550- and 370-kD complexes, which clearly are composed of distinct subunits (Figure 4, middle gel). Further increase of the SDS concentration to 0.04% leads to the generation of several additional subcomplexes, which are separated into vertical rows of subunits upon analysis by 2D BN/SDS-PAGE. Besides the NADH oxidizing 240-, 210-, and 140-kD subcomplexes detected on 1D BN gels, further subcomplexes are visible at 450, 270, 160, and 85 kD.

Subunit Composition of Complex I Subcomplexes from *Arabidopsis*

Subunits of complex I subcomplexes resolved by 2D BN/SDS-PAGE were systematically identified by mass spectrometry (MS)

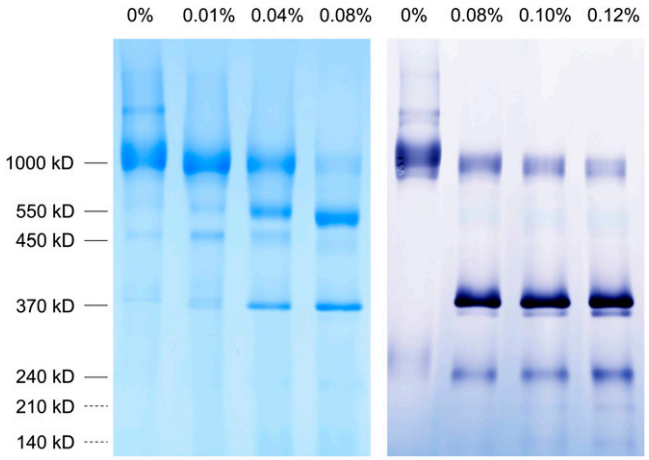

Figure 3. Controlled Disassembly of Complex I from *Arabidopsis* by SDS Treatment.

Purified complex I was treated with different SDS concentrations to induce its dissection into subcomplexes. The fractions were separated via BN-PAGE. Gels were either stained with Coomassie blue colloidal (left) or by an in-gel activity stain for NADH-dehydrogenase (right). Molecular masses are indicated on the left (in kD), and the SDS-concentrations used for complex I disassembly are given on top of the gels.

to determine the protein composition of the subcomplexes (Figure 5). Overall, 50 gel spots were analyzed, representing 40 different complex I subunits and a few contaminating proteins like prohibitin, the β-subunit of ATP synthase (complex V), Ser hydroxymethyltransferase, and lipoamide dehydrogenase (Table 1). Protein determinations revealed that the 550-, 450-, 270-, 160-, and 85-kD subcomplexes are related to the membrane arm (indicated in red on Figure 5) and the 370-, 240-, 210-, and two 140-kD subcomplexes to the peripheral arm (indicated in orange on Figure 5). MS-based protein identifications gave insights into the subunit compositions of 10 different complex I subcomplexes (first given for the peripheral arm and afterwards for the membrane arm).

(1) The 370-kD subcomplex represents the entire peripheral arm. It includes at least 11 subunits: the so-called 75-kD, 51-kD, 49-kD (ND7), 30-kD (ND9), 24-kD, TYKY, B13, PSST, and B8 subunits (bovine nomenclature), the plant-specific subunit At1g67785 (~12 kD), and the previously not described *Arabidopsis* complex I subunit At3g03070 (~10 kD), which is homologous to the 13-kD subunit of the bovine enzyme (Figure 6).

(2) The 240-kD subcomplex represents the so-called NADH oxidation-module (N-module) of the peripheral arm, which previously was identified after pH- and Triton X-100–induced destabilization of complex I isolated from *E. coli* (Leif et al., 1995). It is composed of at least four proteins: the 51-kD subunit, which includes the NADH oxidation domain, the 75-kD subunit, the 24-kD subunit, the B8 subunit, and/or the plant-specific At1g67785 protein.

(3) The slightly smaller 210-kD subcomplex comprises only the three core subunits of the N-module, namely, the 75-, 51-, and 24-kD subunits.

(4) and (5) Careful inspection of the 2D gel in Figure 5 revealed that the 140-kD subcomplex consists of two distinct comigrating subcomplexes termed 140a and 140b. Assignment of subunits to the two subcomplexes is based on spot shape (barbell shaped in the case of subcomplex 140a and round in the case of subcomplex 140b). Subcomplex 140b includes the 51- and 24-kD subunits. Due to the presence of the NADH binding 51-kD subunit, it becomes visible upon in-gel NADH staining like the 240- and 210-kD subcomplexes (Figure 3).

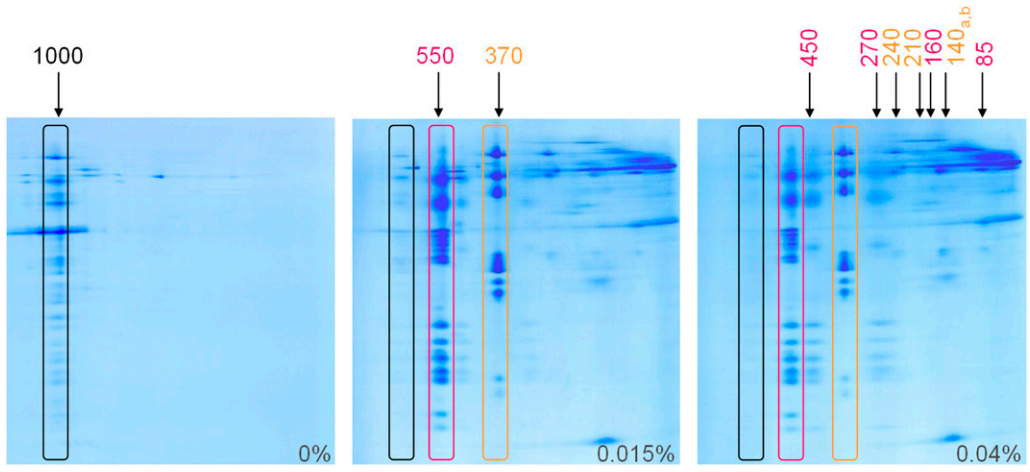

Figure 4. Analysis of Complex I Subcomplexes by 2D Gel Electrophoresis.

Purified complex I was treated with different SDS concentrations as indicated on each gel. Subcomplexes of complex I were separated by 2D BN/SDS-PAGE and visualized by Coomassie blue staining. The holocomplex (1000 kD) is indicated by a black box, and the primarily induced 550-kD subcomplex (representing the membrane arm of complex I) and 370-kD subcomplex (the peripheral arm) are marked by red and orange boxes. Secondary subcomplexes induced by increased destabilization are indicated by arrows above the gel to the right. Their estimated molecular masses are given in orange or red according to their assignment to one of the two primarily induced subcomplexes (see Figures 5 and 8).

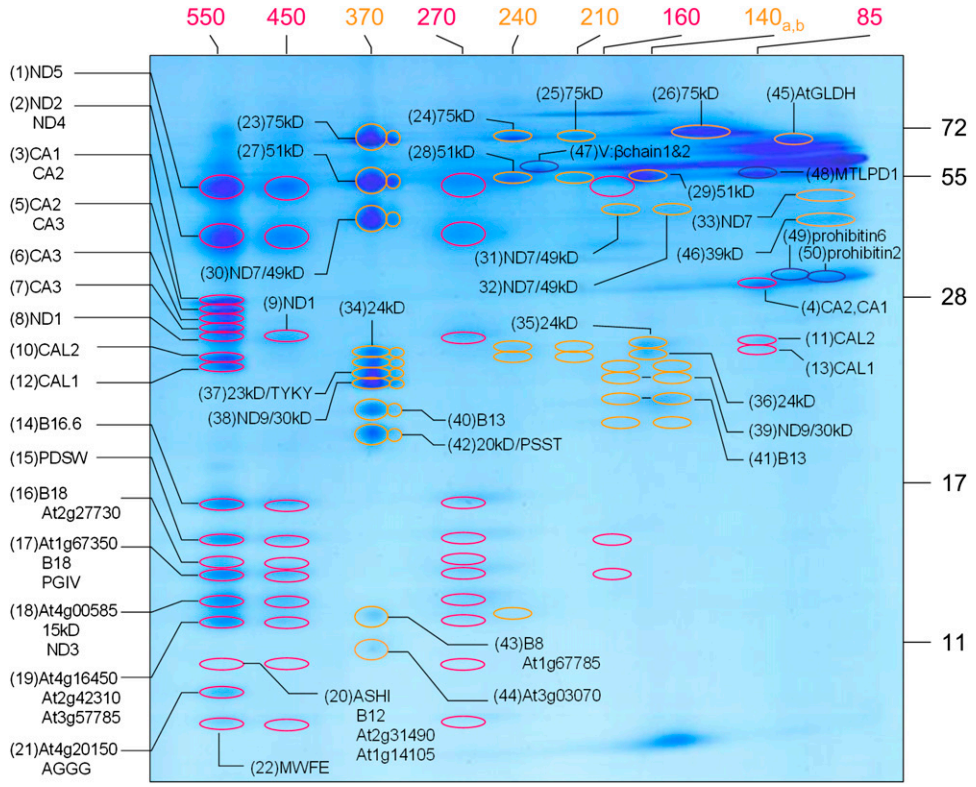

Figure 5. Identification of Subunits of Complex I Subcomplexes by MS.

The complex I fraction was pretreated with 0.04% SDS; subsequently, proteins were resolved by 2D BN/SDS-PAGE. Protein spots were cut out of the gel, digested with trypsin, and analyzed by MS. Spot numbers (in parentheses) refer to those given in Table 1; designations behind the spot numbers correspond to the names of the subunits (see Table 1). Subunits of membrane-embedded complex I subcomplexes are indicated in red, subunits of subcomplexes derived from the peripheral arm in orange, and proteins not belonging to complex I in blue. The sizes of the subcomplexes are indicated above the gel (in kD; red numbers, membrane arm of complex I and subcomplexes; orange, peripheral arm and subcomplexes; 140a,b, two different 140-kD subcomplexes that comigrate on the native gel dimension). The molecular masses of standard proteins are given to the right of the gel.

The 140a subcomplex includes subunits previously reported to form the so-called Q-reduction module (Q-module) of the peripheral arm in *E. coli* (Leif et al., 1995). It is composed of the 49-kD (ND7), 30-kD (ND9), TYKY, PSST, and B13 subunits.

(6) The 550-kD subcomplex represents the membrane arm of *Arabidopsis* complex I. It includes at least 27 subunits, 13 of which are homologous to known subunits of the membrane arm from bovine complex I (ND1, ND2, ND3, ND4, ND5, PDSW, B18, PGIV, 15 kD, B12, ASHI, AGGG, and MWFE). Additionally, the membrane arm of *Arabidopsis* complex I includes a bovine homolog known to be present in the peripheral arm, the so-called 16.6-kD subunit (GRIM19). Thirteen further subunits of the *Arabidopsis* membrane arm are plant-specific proteins, eight of which are rather small and hydrophobic (At4g16450, At2g27730, At2g42310/At3g57785, At4g00585, At4g20150, At2g31490, At1g67350, and the previously not described complex I subunit At5g14105). The five remaining plant-specific subunits of the membrane arm represent the CA subunits CA1, CA2, CA3, CAL1, and CAL2.

(7) The 450-kD subcomplex is a subcomplex of the membrane arm generated most efficiently at a slightly higher SDS concentration. The subunit composition resembles the one of the 550-kD complex, but it lacks all five CA subunits and some of the smaller subunits of the membrane arm.

(8) and (9) The 270- and 160-kD subcomplexes represent smaller forms of the 450-kD subcomplex that lack so far unknown subunits. The 160-kD subcomplex includes the ND5 subunit, the B18 subunit, and/or At2g27730 as well as the PGIV subunit and/or At1g67350.

(10) Finally, an 85-kD subcomplex includes the CA subunits present within plant complex I, the CA1, CA2, CAL1, and CAL2 proteins. Slightly differing horizontal positions of the CAL1 and CAL2 proteins with respect to the CA1 and CA2 subunits indicate that they might not be simultaneously present within individual CA subcomplexes.

The GLDH, which is associated to complex I in plants, and the so-called 39-kD subunit were identified as separate proteins on BN/SDS gels (Figure 5), which do not form part of complex I subcomplexes upon SDS treatment of any concentration and therefore are assumed to be either peripherically localized or at the interphase of the membrane and the peripheral arm.

Elucidation of subunit compositions of complex I subcomplexes allows us to deduce a model of internal subunit arrangement within plant complex I as discussed below.

Table 1. Proteins Identified by MS

Complex I–Related Proteins

Spot[a]	Identity in *Arabidopsis*		Homologs in			Mass (kD)[b]	GRAVY[c]	Score[d]	No MP[e]	Coverage (%)[f]
	Accession No.[g]	Name[h]	*E. coli*	*B. taurus*	*Y. lipolytica*					
1	AtMg00060/AtMg00513/AtMg00665	ND5	NUOL	ND5	NU5M	73.91	0.585	40	5	7
2	AtMg00580	ND4	NUOM	ND4	NU4M	55.23	0.687	7	2	6
	AtMg00285/AtMg01320	ND2	NUON	ND2	NU2M	54.88	0.727	22	3	5
3	At1g47260	CA2	–	–	–	30.07	−0.157	231	21	70
	At1g19580	CA1	–	–	–	29.97	−0.223	82	10	47
4	At1g47260	CA2	–	–	–	30.07	−0.157	216	18	71
	At1g19580	CA1	–	–	–	29.97	−0.223	123	12	53
5	At1g47260	CA2	–	–	–	30.07	−0.157	217	18	70
6	At5g66510.1	CA3	–	–	–	27.84	−0.293	126	11	56
7	At5g66510.1	CA3	–	–	–	27.84	−0.293	208	17	69
8	AtMg00516/AtMg01120/AtMg01275	ND1	NUOH	ND1	NU1M	35.68	0.773	95	2	7
9	AtMg00516/AtMg01120/AtMg01275	ND1	NUOH	ND1	NU1M	35.68	0.773	31	1	4
10	At3g48680	CAL2	–	–	–	27.96	0.041	175	12	51
11	At3g48680	CAL2	–	–	–	27.96	0.041	154	11	46
12	At5g63510	CAL1	–	–	–	27.57	0.06	195	14	58
13	At5g63510	CAL1	–	–	–	27.57	0.06	122	10	49
14	At2g33220	B16.6	–	B16.6	NB6M	16.12	−0.472	932	12	63
15	At3g18410/	PDSW	–	PDSW	NIDM	12.44	−0.956	314	11	83
	At1g49140	PDSW	–	PDSW	NIDM	12.53	−0.88	312	10	78
16	At2g02050	B18	–	B18	NB8M	11.74	−0.428	398	10	73
	At2g27730	At2g27730	–	–	–	11.95	−0.467	266	7	45
17	At2g02050	B18	–	B18	NB8M	11.74	−0.428	408	8	70
	At1g67350	At1g67350	–	–	–	15.25	0.615	299	9	76
	At5g18800/	PGIV	–	PGIV	NUPM	11.97	−0.492	84	2	16
	At3g06310	PGIV	–	PGIV	NUPM	12.16	−0.456	46	2	15
18	At4g00585	At4g00585	–	–	–	9.86	−0.592	142	6	69
	At2g47690	15 kD	–	15 kD	–	13.97	−0.918	49	1	14
	AtMg00990	ND3	NuoA	ND3	NU3M	13.66	0.590	83	2	17
19	At4g16450	At4g16450	–	–	–	11.35	0.024	463	6	61
	At2g42310/	At2g42310	–	–	–	12.63	−0.539	281	4	33
	At3g57785	At3g57785	–	–	–	12.66	−0.521	117	3	29
20	At5g47570	ASHI	–	ASHI	NIAM	13.21	0.061	85	4	24
	At2g02510	B12	–	B12	NB2M	8.05	−0.503	51	1	16
	At2g31490	At2g31490	–	–	–	8.29	−0.5	43	1	12
	At5g14105	At5g14105	–	–	–	8.44	−0.247	36	1	17
21	At4g20150	At4g20150	–	–	–	9.21	−0.2	328	6	83
	At1g76200	AGGG	–	AGGG	–	7.57	−0.536	113	4	55
22	At3g08610	MWFE	–	MWFE	NIMM	7.34	−0.189	31	2	21
23	At5g37510	75 kD	NUOG	75 kD	NUAM	81.18	−0.154	2147	35	52
24	At5g37510	75 kD	NUOG	75 kD	NUAM	81.18	−0.154	154	19	35
25	At5g37510	75 kD	NUOG	75 kD	NUAM	81.18	−0.154	133	16	28
26	At5g37510	75 kD	NUOG	75 kD	NUAM	81.18	−0.154	208	21	35
27	At5g08530	51 kD	NUOF	51 kD	NUBM	53.35	−0.303	226	21	50
28	At5g08530	51 kD	NUOF	51 kD	NUBM	53.35	−0.303	90	9	24
29	At5g08530	51 kD	NUOF	51 kD	NUBM	53.35	−0.303	160	18	35
30	AtMg00510	ND7	NUOD	49 kD	NUCM	44.58	−0.408	83	10	23
31	AtMg00510	ND7	NUOD	49 kD	NUCM	44.58	−0.408	64	10	19
32	AtMg00510	ND7	NUOD	49 kD	NUCM	44.58	−0.408	21	5	13
33	AtMg00510	ND7	NUOD	49 kD	NUCM	44.58	−0.408	48	8	22
34	At4g02580	24 kD	NUOE	24 kD	NUHM	28.39	−0.36	118	10	32
35	At4g02580	24 kD	NUOE	24 kD	NUHM	28.39	−0.36	95	9	31
36	At4g02580	24 kD	NUOE	24 kD	NUHM	28.39	−0.36	120	9	30
37	At1g79010	TYKY	NUOI	TYKY	NUKM	25.50	−0.559	84	9	40
38	AtMg00070	ND9	NUOC	30 kD	NUGM	22.69	−0.676	76	8	42
39	AtMg00070	ND9	NUOC	30 kD	NUGM	22.69	−0.676	78	9	44

(Continued)

Table 1. (continued).

Complex I–Related Proteins

Spot[a]	Identity in *Arabidopsis* Accession No.[g]	Name[h]	Homologs in *E. coli*	*B. taurus*	*Y. lipolytica*	Mass (kD)[b]	GRAVY[c]	Score[d]	No MP[e]	Coverage (%)[f]
40	At5g52840	B13	–	B13	NUFM	19.34	−0.478	119	10	56
41	At5g52840	B13	–	B13	NUFM	19.34	−0.478	116	9	42
42	At5g11770	PSST	NUOB	PSST	NUKM	24.04	−0.123	106	7	33
43	At5g47890	B8	–	B8	NI8M	10.85	−0.289	67	5	59
	At1g67785	At1g67785	–	–	–	7.53	−0.417	35	2	36
44	At3g03070	13 kD	–	13 kD	NUMM	12.23	−0.246	268	4	43
45	At3g47930	GLDH	–	–	–	68.56	−0.479	91	11	30
46	At2g20360	39 kD	–	39 kD	NUEM	43.94	−0.059	192	17	44

Other Proteins

Spot[a]	Accession No.[g]	Name	Mass (kD)[b]	GRAVY[c]	Score[d]	No MP[e]	Coverage (%)[f]
47	At5g08670/At5g08690	β-Subunit of the mitochondrial ATP-synthase	59.63	−0.152	133	16	33
	At5g26780	Ser-hydroxymethyltransferase 2 (SMH2)	57.34	−0.286	95	14	32
48	At1g48030	Mitochondrial lipoamide DH1 (MTLPD1)	53.99	−0.042	170	23	55
	At3g17240	Mitochondrial lipoamide DH2 (MTLPD2)	53.99	−0.023	130	20	54
49	At2g20530	Prohibitin 6 (AtPHB6)	31.62	−0.140	68	7	32
50	At1g03860	Prohibitin 2 (AtPHB2	31.79	−0.155	95	13	62

[a]Spot number in accordance with Figure 5. In some cases, more than one complex I subunit was found to be present within a single spot. Furthermore, in some cases, individual subunits of complex I were identified twice in neighboring spots. This is interpreted to be due to spot overlappings on the gel. In most cases, identification of a subunit was most significant for one single spot, allowing unambiguous assignment of spots and subunits.

[b]Calculated molecular mass of the identified protein as deduced from the corresponding gene.

[c]GRAVY (grand average of hydropathy) score of the protein.

[d]Probability score for the protein identification based on MS analysis and MASCOT search.

[e]Number of unique matching peptides.

[f]Sequence coverage of a protein by identified peptides.

[g]Accession numbers as given by TAIR (http://www.Arabidopsis.org/). More than one accession number is given in case a subunit is encoded by more than one gene in identical form. In some cases, subunits are present in isoforms. Accessions for all isoforms exactly matching to identified peptides are given. Note that in some cases the identified peptides do not allow us to distinguish between possible isoforms.

[h]Subunits of complex I from *Arabidopsis* are named according to the bovine nomenclature. Subunits specific to complex I of plant mitochondria are named according to the corresponding genes annotated by TAIR (www.Arabidopsis.org). Exceptions: the plant-specific CA subunits are named CA1, CA2, CA3, CAL1, and CAL2, and the L-galactone-1,4-lactone dehydrogenase is named GLDH in accordance with the literature. Furthermore, *Arabidopsis* homologs to the 30- and 49-kD subunits of bovine complex I are designated ND9 and ND7 because the corresponding proteins are encoded by the mitochondrial genome in plants.

DISCUSSION

Biochemical Procedures to Characterize Complex I

A protocol for complex I isolation is presented that is based on mitochondrial preparation, sucrose gradient ultracentrifugation, and depletion of complex III–related contaminants by cytochrome c affinity chromatography. Protocols previously published for the isolation of complex I from plants include ion-exchange or immunoaffinity chromatography, which require salt gradients or acid treatment for complex I elution (Leterme and Boutry, 1993; Herz et al., 1994; Rasmusson et al., 1994; Trost et al., 1995; Combettes and Grienenberger, 1999). By contrast, the protocol presented here completely avoids high salt conditions since complex I passes the cytochrome c affinity column used for complex III depletion in the flow-through fraction. Complex I therefore can be expected to have optimal integrity for further structural analysis.

Insights into the internal subunit arrangement of complex I were obtained by its careful disassembly and biochemical analysis of the generated disassembly products. Incubation of complex I with low concentrations of SDS proved to be an ideal tool for careful subcomplex generation. It is textbook knowledge that SDS treatment of biochemical fractions is incompatible with native protein characterization. However, SDS concentrations usually employed in protein science often are in the range of 1% or higher (e.g., 5% for sample preparation prior to SDS-PAGE) (Laemmli, 1970; Schägger and von Jagow, 1987). Here, we report use of very low SDS concentrations in the range of 0.01 to 0.04%. Indeed, low SDS conditions cause very distinct

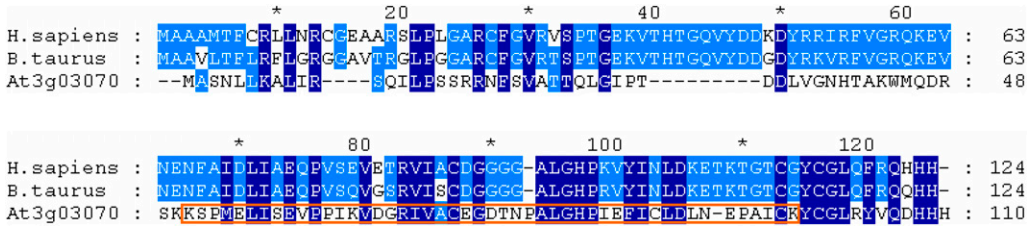

Figure 6. Alignment of At3g03070 with the 13-kD Subunit of Human and Beef Complex I.

Amino acid positions identical in all three sequences are highlighted in dark blue and amino acid positions conserved in two sequences in light blue. The orange box indicates peptides identified by MS analyses.

dissection of complex I into functional modules in a highly reproducible way. There are a few examples in the literature on usage of low SDS for native protein analyses, for example, the green native gel electrophoresis system developed for the analysis of protein complexes of the photosynthesis apparatus, which is based on a first gel dimension in the presence of low and a second gel dimension in the presence of high SDS (Thornber, 1986; Allen and Staehelin, 1991). We suggest the use of low SDS concentrations generally as a tool for the biochemical analysis of the internal architecture of protein complexes.

Subunits of Mitochondrial Complex I from *Arabidopsis*

Forty different complex I subunits were identified by MS analysis of complex I subcomplexes (Figure 5, Table 1). Compared with the most extensive study on complex I subunits in plants (Meyer et al., 2008), which was based on the separation of complex I proteins by three-dimensional BN/SDS/SDS-PAGE, six subunits were not detected (the ND6, 18-kD, B17.2, B14.7, B14, and At1g68680 subunits). These subunits probably are lost during low SDS treatment. Indeed, at least five subunits with apparent molecular masses of 39, 19, 16, 8, and 7 kD form part of intact complex I on BN gels but neither are part of the membrane nor the peripheral arm (see Supplemental Figure 1 online). The 39-kD subunit was identified by MS on the 2D BN/SDS gel shown in Figure 5 as a monomer, whereas the other subunits were not detected. On the other hand, four of the 40 subunits identified in our study were not reported in Meyer et al. (2008): the homolog of the bovine 13-kD subunit (At4g03070; Figure 6), ND3, GLDH, and the novel plant-specific subunit At1g14105. Two further complex I subunits (B22 and At1g14450) were identified by another study (Sunderhaus et al., 2006) but not found by Meyer et al. (2008) or within any of the complex I subcomplexes analyzed in this investigation. Overall, 17 plant-specific complex I subunits have now been identified (Heazlewood et al., 2003; Sunderhaus et al., 2006; Meyer et al., 2008; this study). Except for the CA subunits and GLDH, most of them are small hydrophobic subunits forming part of the membrane arm. It currently cannot be excluded that some of these proteins are structural homologs of small subunits additionally present in fungal or mammalian complex I since sequence conservation often is low between related proteins if they are small and hydrophobic (Brandt, 2006).

In addition to the overall 48 MS-identified complex I subunits of *Arabidopsis* (Sunderhaus et al., 2006; Meyer et al., 2008; this study), the mitochondrial genome of *Arabidopsis* encodes an ND4L homolog that is extremely hydrophobic and most likely difficult to detect by MS. The number of distinct complex I subunits in *Arabidopsis* therefore adds up to at least 49. Bovine complex I, which is the largest complex I particle biochemically characterized so far, has 45 distinct subunits (Carroll et al., 2006), and complex I of the fungus *Yarrowia lipolytica* has 40 subunits (Morgner et al., 2008). Indeed, upon direct size comparison of bovine and potato (*Solanum tuberosum*) complex I by 1D BN-PAGE, the enzyme complex from plants is slightly larger (Jänsch et al., 1995).

For several subunits, pairs of isoforms occur in *Arabidopsis*. MS analysis allowed us to detect isoforms for the PSDW subunit (encoded by At3g18410 and At1g49140), the PGIV subunit (At5g18800 and At3g06310), and a 12.6-kD subunit (At2g42310 and At3g57785; Table 1). For some other subunits, genes encoding isoforms are present in the *Arabidopsis* genome, but the encoded proteins are not distinguishable by the peptide sequences obtained.

The CA Subunits of Complex I from *Arabidopsis*

The CA1, CA2, CA3, CAL1, and CAL2 proteins also exhibit sequence similarity and might be considered to represent isoforms. However, biochemical evidence indicates the presence of at least three proteins of the CA/CAL family in individual complex I particles because the CA domain attached to complex I has a trimeric structure (Sunderhaus et al., 2006). Unfortunately, despite large efforts, the CA/CAL proteins so far could not be functionally characterized. The genes encoding CA1 and CA2 are downregulated if plants are cultivated in the presence of high CO_2 concentrations (Perales et al., 2005), which is also known for enzymes involved in photorespiration. A role for the CA/CAL proteins in an intracellular CO_2 transfer mechanism from mitochondria to chloroplasts analogous to the cyanobacterial carbon concentration mechanism has been proposed (Braun and Zabaleta, 2007). Recently, overexpressed CA2 was shown to bind CO_2 and/or bicarbonate efficiently (Martin et al., 2009).

For reasons not understood, the five CA/CAL proteins are represented by six protein spots on 2D BN/SDS gels (Figure 5). Since they partially overlap, assignment of the spots to the proteins is difficult. However, the most likely explanation is that CA3 occurs in two versions of ~28 and 29 kD. Interestingly, the corresponding gene also is annotated in two versions (At5g66510.1 and At5g66510.2), which differ in size by ~1.2

kD (27.837 and 29.043 kD) due to a small insertion in At5g66510.2 at a central position. The functional relevance of this possible CA3 heterogeneity is so far unclear.

Mapping of MS-identified peptides for the CA/CAL proteins to the complete amino acid sequences deduced from the corresponding genes indicates the absence of a cleavable presequence for CA1, CA2, and CA3 (Figure 7). In the case of CA3, the N terminus of the primary translation product forms part of the mature protein. For CA1 and CA2, the most N-terminal peptides identified by MS start at amino acid 7 of the translation products. The six N-terminal amino acids of the translation products do not exhibit the typical properties of cleavable mitochondria targeting sequences (Glaser et al., 1998). Also, the apparent molecular masses of CA1 and CA2, which both migrate at 30 kD on 2D BN/SDS gels, exactly fit to the calculated molecular masses of the translation products (29.970 and 30.065 kD). By contrast, the CAL1 and CAL2 sequences have cleavable presequences. Removal of the targeting sequences was previously shown by an in vitro processing assay (Perales et al., 2004). The length of the presequences can be predicted to be 22 amino acids for CAL1 and 26 amino acids for CAL2 on the basis of a sequence comparison to the N-terminal region of a homologous 29-kD subunit of complex I from potato (Herz et al., 1994) (Figure 7). Also, N termini for the mature CAL2 and CAL1 proteins were recently directly determined by an elegant MS-based approach (Huang et al., 2009). The resulting masses of the mature CAL1 and CAL2 subunits are 25.079 and 25.045 kD, which nicely corresponds to their apparent masses upon separation by BN/SDS-PAGE (Figure 5).

Internal Architecture of Complex I from *Arabidopsis*

Incubation of isolated complex I from *Arabidopsis* with SDS solutions of low concentration allows the dissection of the complex into 10 defined subcomplexes. At 0.01% SDS, the membrane arm (550 kD) and the peripheral arm (370 kD) are generated. Furthermore, approximately five subunits are detached as monomers during this first dissection step, including the 39-kD subunit, which was identified by MS within the dye front of the BN gel dimension. Increase of SDS to 0.04% further dissects the two arms into secondary subcomplexes of 450, 270, 240, 210, 160, 140, 140, and 85 kD. The proposed disassembly process of complex I from *Arabidopsis* is summarized in Figure 8. Apparent molecular masses of the subcomplexes are in good accordance with calculated masses of the subcomplexes based on the sum of the masses of their subunits. However, in some cases, the calculated masses of the subcomplexes are slightly lower, most likely indicating that further subunits might additionally be present, which are not resolved on the Coomassie blue–stained gel (Figure 5).

Subfractionation procedures were previously used for the analysis of complex I particles from other organisms. In beef, treatment of isolated complex I with the nondenaturating detergent *N*,*N*-dimethyldodecylamine *N*-oxide dissociates the enzyme

Figure 7. Coverage of the CA Sequences by Peptides Identified by MS.

The five amino acid sequences of the CA/CA-like subunits of *Arabidopsis* complex I were aligned using ClustalW2 (http://www.ebi.ac.uk/Tools/clustalw2/index.html). Identified peptides are highlighted in blue. The sequences correspond to the following accessions: At1g19580 (CA1), At1g47260 (CA2), At5g66510.1 (CA3), At5g63510 (CAL1), and At3g48680 (CAL2). The red arrow indicates the cleavage site for the removal of the presequences in CAL1 and CAL2.

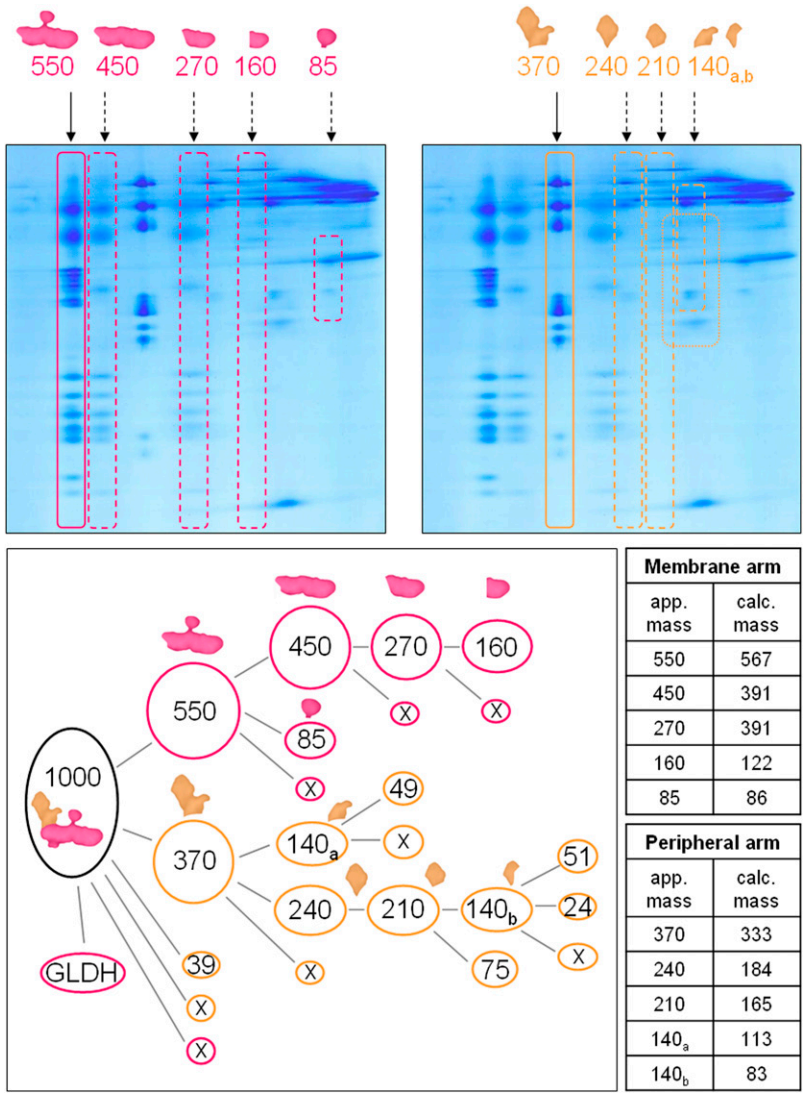

Membrane arm	
app. mass	calc. mass
550	567
450	391
270	391
160	122
85	86

Peripheral arm	
app. mass	calc. mass
370	333
240	184
210	165
140_a	113
140_b	83

Figure 8. Proposed Disassembly Process for *Arabidopsis* Complex I.

Top: 2D BN/SDS separations of complex I subcomplexes generated by 0.04% SDS. The membrane arm and its dissection products are indicated on the 2D gel on the left and the peripheral arm and its subcomplexes on the 2D gel to the right. Apparent molecular masses of the subcomplexes are given above the gels (in kD). Bottom: proposed disassembly pathway of *Arabidopsis* complex I. Membrane subcomplexes/subunits are given in red and the ones of the peripheral arm in orange. Numbers indicate apparent molecular masses (in kD). The table to the right of the scheme compares the apparent molecular masses of the generated complex I subcomplexes with the calculated molecular mass of the sum of their protein subunits identified by MS. Since two subcomplexes deduced from the peripheral arm have apparent molecular masses of 140 kD, these are distinguished in the figure and in the table by (a) and (b). For unknown reasons, the calculated molecular mass of the 270 kD complex is too high.

into two parts, an α-part including the subunits of the peripheral arm as well as adjacent subunits of the membrane arm and a β-part that represents the remaining membrane arm (Finel et al., 1992). Modified procedures allow the purification of a λ-subcomplex including the hydrophilic subunits and a γ-subcomplex that includes the more hydrophobic subunits of the α-part of beef complex I (Arizmendi et al., 1992; Sazanov et al., 2000; Carroll et al., 2003). In *E. coli*, treatment of complex I with Triton X-100 leads to the dissociation of complex I into a membrane part, a water-soluble NADH dehydrogenase part, and an amphipathic part that connects the two other parts (Leif et al., 1995). The subunit compositions of the bovine and *E. coli* subcomplexes have been resolved (Leif et al., 1995; Carroll et al., 2003). Based on the protein composition of complex I subcomplexes, functional domains have been defined (reviewed in Brandt, 2006): an NADH oxidation (N) module, a quinone reduction (Q) module, and a proton translocating (P) module.

Systematic analysis of the subunit compositions of the 10 complex I subcomplexes generated by SDS treatment gave the following insights into the internal architecture of this protein

complex in *Arabidopsis* (summarized in Figure 9). The 240-kD subcomplex (75-kD, 51-kD, 24-kD, and B8 and/or At1g67785 subunits) represents the N-module and the 140-kD (140a) subcomplex (49-kD/ND7, 30-kD/ND9, TYKY, PSST, and B13 subunits) the Q-module of complex I. Together with the 13-kD subunit (At3g03070), they form the peripheral arm (370 kD). The 240-kD subcomplex can be further dissected into a smaller 140-kD (140b) subcomplex including the 51- and 24-kD subunits and possibly some further subunits. This is the smallest subcomplex exhibiting NADH oxidation activity (Figure 3).

The membrane arm subcomplex (550 kD) includes at least five of the hydrophobic mitochondrially encoded subunits (ND1, ND2, ND3, ND4, and ND5), seven further mainly hydrophobic subunits homologous to nuclear-encoded complex I subunits from beef, eight additional plant-specific subunits, and the five CA/CAL proteins (Figure 9). Arrangement of all these subunits within the membrane arm still is largely unknown because the generation of secondary subcomplexes is difficult. However, based on single particle EM and cross-linking experiments, the location for some proteins is known. For instance, several lines of evidence suggest that the ND4 and ND5 proteins are in close proximity and form the tip of the membrane arm (Holt et al., 2003; Baranova et al., 2007a, 2007b). Analysis of a 210-kD subcomplex derived from the membrane arm of complex I from *Arabidopsis* indicates an association of the PDSW subunit and at least one of the three subunits included in spot 17 (Figure 5, Table 1) with ND5. The ND6 and possibly also the ND4L subunits, which could not be identified within the 550-kD membrane arm of *Arabidopsis* complex I, probably are detached from complex I during initial dissection into the membrane and the peripheral arm at 0.01% SDS and are speculated to represent the end of the membrane arm at the site of its connection to the peripheral arm. This is in line with detection of ND6 in subcomplex α of complex I from beef but its absence in subcomplex λ (Carroll et al., 2003). Most interestingly, the B16.6 subunit, which is identical to the GRIM-19 protein involved in apoptosis, forms part of the membrane arm of complex I in *Arabidopsis* but was reported to be part of the peripheral (λ) arm in beef (Carroll et al., 2003). This most likely points to a location of B16.6 at the intersection of the two complex I arms.

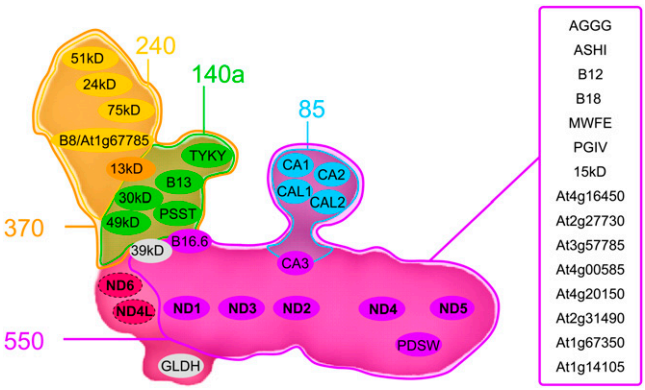

Figure 9. Model of the Internal Architecture of Mitochondrial Complex I from *Arabidopsis*.

Based on the presented disassembly analysis and subunit identifications, the 550-, 370-, 240-, 140-, and 85-kD subcomplexes are assigned to the EM average structure of complex I (Figure 1). The approximate localization of subunits within the subcomplexes is given in accordance with further insights based on the presented findings and data available in the literature (Sazanov and Hinchliffe, 2006; Baranova et al., 2007a, 2007b; Zickermann et al., 2009). The localization of several subunits within the membrane arm of complex I so far is unknown (subunits included in box to the right of the model).

Some subunits were detached from *Arabidopsis* complex I during initial dissociation of the peripheral and the membrane arm (e.g., the 39-kD subunit). However, in a previous investigation (Sunderhaus et al., 2006), this protein was reported to be associated with the peripheral arm in *Arabidopsis*. Also, GLDH, which only in plants is part of complex I (Heazlewood et al., 2003), was not found to be associated with either of its two arms. Since this enzyme catalyzes the terminal step of ascorbic acid biosynthesis, it should be associated with the membrane arm of complex I on the side exposed to the intermembrane space. However, recent findings indicate that GLDH might represent an assembly factor important for complex I biogenesis (Pineau et al., 2008). Indeed, GLDH initially was described as a subunit of an *Arabidopsis* complex I version of slightly reduced molecular mass (Heazlewood et al., 2003; Millar et al., 2003).

Finally, an 85-kD subcomplex is generated if the membrane arm is further destabilized using 0.04% SDS. This complex includes the 30-kD CA1 and CA2 proteins and the 25-kD CAL1 and CAL2 proteins. Based on previous findings that CAs are trimers, we conclude that probably three of the four proteins form a CA domain. The stoichiometry of the four proteins upon analysis by 2D BN/SDS-PAGE (Figure 5) differs: the amount of CA1+CA2 clearly exceeds the one of CAL1+CAL2. We speculate that the CA domain attached to complex I might include two CA proteins (CA1+CA2 or two copies of CA2 or two copies of CA1) and additionally either CAL1 or CAL2. Interestingly, interaction of CA2 with CAL1 and CAL2 was previously proved by a two-hybrid screen (Perales et al., 2004). Furthermore, using the same approach, it was shown that the N-terminal half of CA2 binds to the CAL subunits. By contrast, CA1–CA2 interaction has not been reported. For reasons currently not understood, CA3 was not found to interact with any of the other members of the CA/CAL protein family, neither by two-hybrid screening nor by MS analysis of complex I subcomplexes. Further investigations will be necessary to better understand the composition and function of the CA domain of plant complex I.

Outlook

The presented biochemical strategy, SDS-mediated dissection of isolated complex I, separation of subcomplexes by BN/SDS-PAGE, and protein identifications by MS, allowed us to achieve insights into the internal architecture of complex I. Since crystallization of the entire complex proved to be intractable, sophisticated biochemical procedures are required to better understand the structure and function of this key enzyme complex of the respiratory chain. Despite large efforts, knowledge on the subunit arrangements within the membrane arm of eukaryotic complex I still is fragmentary. New protocols to generate

additional subcomplexes of this arm will be crucial for a deeper understanding of internal complex I structure. Further progress could also come from combining controlled complex I dissections and cross-link approaches in future experiments. Analysis of complex I certainly will remain one of the most fascinating challenges in biochemistry.

METHODS

Arabidopsis thaliana Cultivation and Isolation of Mitochondria

Cell cultures of *Arabidopsis* wild type (Columbia-0) were established as described by May and Leaver (1993). Cells were cultivated in a suspension culture maintained as outlined previously (Sunderhaus et al., 2006). Mitochondria were isolated from *Arabidopsis* suspension culture as given by Werhahn et al. (2001).

Purification of Complex I

Purification of complex I from isolated *Arabidopsis* mitochondria followed a two-step procedure based on (1) sucrose gradient ultracentrifugation to prepare the ~1-MD protein fraction and (2) cytochrome c affinity chromatography to deplete the complex I–enriched 1-MD fraction from remaining contaminations of complex III_2 and supercomplex $I+III_2$.

Isolated mitochondria were pelleted by centrifugation and resuspended in digitonin solubilization buffer (30 mM HEPES, 150 mM potassium acetate, 10% [v/v] glycerol, and 5% [w/v] digitonin) at a detergent/protein ratio of 5 mg/mg. Protein complexes were subsequently resolved by sucrose gradient ultracentrifugation. Solubilized mitochondria (~10 mg mitochondrial protein) were loaded onto a 12-mL sucrose gradient (15 mM Tris, 20 mM KCl, 0.2% [w/v] digitonin, and 0.3 to 1.5 M sucrose). Ultracentrifugation was performed at 4°C using Beckmann 9/16 × 3 3/4 Ultra Clear Tubes and the Beckmann SW40Ti rotor (146.000*g* for 20 h). Afterwards, the gradient was divided into 700-μL fractions, and the protein complex composition of each fraction was analyzed by 1D BN-PAGE (see below). Fractions containing complex I but devoid of complex V were used for a cytochrome c–mediated depletion of complex III contaminations.

For this approach, cytochrome c was coupled to CNBr-activated Sepharose as described by Weiss and Juchs (1978). Before usage, the cytochrome c sepharose was washed with 300 mL oxidation solution (5 mM $K_3[Fe(CN)_6]$, 0.5% [v/v] Triton X-100, 0.1 M $NaHCO_3$, and 0.5 M NaCl) to oxidize the cytochrome c. Subsequently, this solution was removed by washing the Sepharose with 150 mL washing buffer (20 mM Tris-acetate, pH 7.0, 5% [w/v] sucrose, 0.04% [w/v] digitonin, and 0.2 mM PMSF). Six milliliters of Sepharose was filled into a column (1 cm × 10 cm) and washed with washing buffer another time. Afterwards, the complex I–containing sucrose gradient fractions were transferred on the top of the column, and the flow-through was collected in 1-mL fractions. Additional 2 mL of washing buffer was used to remove remaining complex I from the column. Finally, complex III_2 and the $I+III_2$ supercomplex were eluted from the column using a salt gradient (20 to 200 mM Tris-acetate, pH 7.0, 5.0% [w/v] sucrose, 0.04% [w/v] digitonin, 0.2 mM PMSF, and 2 mM Na-ascorbate). The eluate was collected in 1-mL fractions. For evaluation of the protein complex content of the fractions, 25 μL of each flow-through fraction and 75 μL of each eluate fraction were analyzed by 1D BN-PAGE (see below). Fractions containing pure complex I were concentrated using an ultra filtration cell (Millipore; polyethersulfone filter; exclusion limit, 100.000 kD) to a final protein concentration of ~5 mg/mL.

Controlled Disassembly of Complex I

For disassembly experiments, purified complex I (1 mg in 200 μL) was treated with low concentrations of SDS (0.01 to 0.12% [w/v]) for 5 min on ice. Afterwards, 1 μL BN loading buffer (750 mM aminocaproic acid and 5% [w/v] Coomassie Brilliant Blue G 250) was added.

Gel Electrophoresis Procedures

1D BN-PAGE was used to separate the generated complex I subcomplexes and 2D BN/SDS-PAGE to analyze their subunit composition. Procedures were performed as outlined previously (Wittig et al., 2006). Proteins were either visualized by Coomassie Brilliant Blue colloidal staining (Neuhoff et al., 1988) or in-gel NADH dehydrogenase activity staining (Zerbetto et al., 1997).

MS

Tryptic digestion of proteins was performed as follows: Protein spots were cut from 2D BN/SDS gels and destained. Gel pieces were dehydrated using acetonitrile. For alkylation of cysteins, gel pieces were first incubated with 20 mM DTT for 30 min at 56°C, dehydrated, and incubated in 55 mM iodoacetamide at room temperature for the same time in the dark. The dehydrated gel pieces were incubated in 0.1 M NH_4HCO_3, and digestion was performed at 37°C overnight using trypsin (2 μg/mL resuspension buffer [Promega] in 0.1 M NH_4HCO_3). Tryptic peptides were extracted by incubation with acetonitrile for 15 min at 37°C. Supernatants were kept and basic peptides were extracted with 5% formic acid for 15 min at 37°C. The dehydration step was repeated, and the supernatant was pooled with the first one. Extracted peptides were finally dried via vacuum centrifugation and stored at −20°C.

Protein identification by MS was performed as follows: Tryptic peptides were resuspended in 20 μL of washing solution (2% [v/v] methanol and 0.5% [v/v] formic acid) and desalted using ZipTips (0.2 μL C_{18}; Millipore). For matrix-assisted laser desorption ionization (MALDI) analyses, 1 μL of Matrix solution (0.1% [w/v] α-Cyano-4-hydroxy-cinnamic acid, 25% [v/v] acetonitrile, and 0.1% [w/v] triflouroacetic acid) was mixed with 1 μL of desalted peptide solution and spotted on a MALDI target. MALDI-time of flight (TOF)/TOF-MS analyses were performed with an Ultraflex II mass spectrometer (Bruker Daltonics). Offline electrospray ionization (ESI)-quadrupole (Q)-TOF-MS analyses were performed with a Q-TOF 2 mass spectrometer (Waters).

For liquid chromatography–ESI-Q-TOF-MS analyses, tryptic peptides were resuspended in 15 μL 0.1% [v/v] formic acid. The MS analyses were performed with the EASY-nLC System (Proxeon) coupled to a MicrOTOF-Q II mass spectrometer (Bruker Daltonics).

Proteins were identified using the MASCOT search algorithm against (1) the *Arabidopsis* protein database (www.Arabidopsis.org; release TAIR 8), (2) a complex I database generated from the complex I subunits identified by Meyer et al. (2008), and (3) the NCBI nonredundant protein database (www.ncbi.nih.gov).

Accession Numbers

All peptides identified in our study match protein sequences deduced from the *Arabidopsis* genome sequence (www.Arabidopsis.org). The corresponding accession numbers are listed in Table 1 (column 2).

Supplemental Data

The following materials are available in the online version of this article.

Supplemental Figure 1. Subunits Detached from Complex I upon Treatment with Low Concentrations of SDS.

ACKNOWLEDGMENT

This research was supported by the Deutsche Forschungsgemeinschaft (Grant Br 1829/10-1).

Received December 23, 2009; revised February 12, 2010; accepted February 18, 2010; published March 2, 2010.

REFERENCES

Abdrakhmanova, A., Zickermann, V., Bostina, M., Radermacher, M., Schägger, H., Kerscher, S., and Brandt, U. (2004). Subunit composition of mitochondrial complex I from the yeast *Yarrowia lipolytica.* Biochim. Biophys. Acta **1658:** 148–156.

Alber, B.E., and Ferry, J.G. (1994). A carbonic anhydrase from the archaeon *Methanosarcina thermophila*. Proc. Natl. Acad. Sci. USA **91:** 6909–6913.

Allen, K.D., and Staehelin, L.A. (1991). Resolution of 16 to 20 chlorophyll-protein complexes using a low ionic strength native green gel system. Anal. Biochem. **194:** 214–222.

Arizmendi, J.M., Skehel, J.M., Runswick, M.J., Fearnley, I.M., and Walker, J.E. (1992). Complementary DNA sequences of two 14.5 kDa subunits of NADH:ubiquinone oxidoreductase from bovine heart mitochondria. Completion of the primary structure of the complex? FEBS Lett. **313:** 80–84.

Baranova, E.A., Holt, P.J., and Sazanov, L.A. (2007b). Projection structure of the membrane domain of *Escherichia coli* respiratory complex I at 8 A resolution. J. Mol. Biol. **366:** 140–154.

Baranova, E.A., Morgan, D.J., and Sazanov, L.A. (2007a). Single particle analysis confirms distal location of subunits NuoL and NuoM in *Escherichia coli* complex I. J. Struct. Biol. **159:** 238–242.

Berrisford, J.M., and Sazanov, L.A. (2009). Structural basis for the mechanism of respiratory complex I. J. Biol. Chem. (in press).

Böttcher, B., Scheide, D., Hesterberg, M., Nagel-Steger, L., and Friedrich, T. (2002). A novel, enzymatically active conformation of the *Escherichia coli* NADH:ubiquinone oxidoreductase (complex I). J. Biol. Chem. **277:** 17970–17977.

Brandt, U. (2006). Energy converting NADH:quinone oxidoreductase (complex I). Annu. Rev. Biochem. **75:** 69–92.

Braun, H.P., and Schmitz, U.K. (1992). Affinity purification of cytochrome c reductase from plant mitochondria. Eur. J. Biochem. **208:** 761–767.

Braun, H.P., and Zabaleta, E. (2007). Carbonic anhydrase subunits of the mitochondrial NADH dehydrogenase complex (complex I) in plants. Physiol. Plant. **129:** 114–122.

Bultema, J.B., Braun, H.P., Boekema, E.J., and Kouril, R. (2009). Megacomplex organization of the oxidative phosphorylation system by structural analysis of respiratory supercomplexes from potato. Biochim. Biophys. Acta **1787:** 60–67.

Cardol, P., Vanrobaeys, F., Devreese, B., Van Beeumen, J., Matagne, R.F., and Remacle, C. (2004). Higher plant-like subunit composition of mitochondrial complex I from *Chlamydomonas reinhardtii*: 31 conserved components among eukaryotes. Biochim. Biophys. Acta **1658:** 212–224.

Carroll, J., Fearnley, I.M., Shannon, R.J., Hirst, J., and Walker, J.E. (2003). Analysis of the subunit composition of complex I from bovine heart mitochondria. Mol. Cell. Proteomics **2:** 117–126.

Carroll, J., Fearnley, I.M., Skehel, J.M., Shannon, R.J., Hirst, J., and Walker, J.E. (2006). Bovine complex I is a complex of 45 different subunits. J. Biol. Chem. **281:** 32724–32727.

Clason, T., Ruiz, T., Schägger, H., Peng, G., Zickermann, V., Brandt, U., Michel, H., and Radermacher, M. (2010). The structure of eukaryotic and prokaryotic complex I. J. Struct. Biol. **169:** 81–88.

Clason, T., Zickermann, V., Ruiz, T., Brandt, U., and Radermacher, M. (2007). Direct localization of the 51 and 24 kDa subunits of mitochondrial complex I by three-dimensional difference imaging. J. Struct. Biol. **159:** 433–442.

Combettes, B., and Grienenberger, J.M. (1999). Analysis of wheat mitochondrial complex I purified by a one-step immunoaffinity chromatography. Biochimie **81:** 645–653.

Dudkina, N.V., Eubel, H., Keegstra, W., Boekema, E.J., and Braun, H.P. (2005). Structure of a mitochondrial supercomplex formed by respiratory chain complexes I and III. Proc. Natl. Acad. Sci. USA **102:** 3225–3229.

Dutilleul, C., Garmier, M., Noctor, G., Mathieu, C., Chétrit, P., Foyer, C.H., and De Paepe, R. (2003). Leaf mitochondria modulate whole cell redox homeostasis, set antioxidant capacity, and determine stress resistance through altered signaling and diurnal regulation. Plant Cell **15:** 1212–1226.

Eubel, H., Jänsch, L., and Braun, H.P. (2003). New insights into the respiratory chain of plant mitochondria. Supercomplexes and a unique composition of complex II. Plant Physiol. **133:** 274–286.

Finel, M., Skehel, J.M., Albracht, S.P., Fearnley, I.M., and Walker, J.E. (1992). Resolution of NADH:ubiquinone oxidoreductase from bovine heart mitochondria into two subcomplexes, one of which contains the redox centers of the enzyme. Biochemistry **31:** 11425–11434.

Friedrich, T., and Böttcher, B. (2004). The gross structure of the respiratory complex I: A Lego system. Biochim. Biophys. Acta **1608:** 1–9.

Glaser, E., Sjöling, S., Tanudji, M., and Whelan, J. (1998). Mitochondrial protein import in plants. Signals, sorting, targeting, processing and regulation. Plant Mol. Biol. **38:** 311–338.

Grigorieff, N. (1998). Three-dimensional structure of bovine NADH: ubiquinone oxidoreductase (complex I) at 22 Å in ice. J. Mol. Biol. **277:** 1033–1046.

Guénebaut, V., Schlitt, A., Weiss, H., Leonard, K., and Friedrich, T. (1998). Consistent structure between bacterial and mitochondrial NADH:ubiquinone oxidoreductase (complex I). J. Mol. Biol. **276:** 105–112.

Guénebaut, V., Vincentelli, R., Mills, D., Weiss, H., and Leonard, K.R. (1997). Three-dimensional structure of NADH-dehydrogenase from *Neurospora crassa* by electron microscopy and conical tilt reconstruction. J. Mol. Biol. **265:** 409–418.

Heazlewood, J.L., Howell, K.A., and Millar, A.H. (2003). Mitochondrial complex I from Arabidopsis and rice: Orthologs of mammalian and fungal components coupled with plant-specific subunits. Biochim. Biophys. Acta **1604:** 159–169.

Herz, U., Schröder, W., Liddell, A., Leaver, C.J., Brennicke, A., and Grohmann, L. (1994). Purification of the NADH:ubiquinone oxidoreductase (complex I) of the respiratory chain from the inner mitochondrial membrane of *Solanum tuberosum*. J. Biol. Chem. **269:** 2263–2269.

Hinchliffe, P., and Sazanov, L.A. (2005). Organization of iron-sulfur clusters in respiratory complex I. Science **309:** 771–774.

Hirst, J., Carroll, J., Fearnley, I.M., Shannon, R.J., and Walker, J.E. (2003). The nuclear encoded subunits of complex I from bovine heart mitochondria. Biochim. Biophys. Acta **1604:** 135–150.

Holt, P.J., Morgan, D.J., and Sazanov, L.A. (2003). The location of NuoL and NuoM subunits in the membrane domain of the *Escherichia coli* complex I: Implications for the mechanism of proton pumping. J. Biol. Chem. **278:** 43114–43120.

Huang, S., Taylor, N.L., Whelan, J., and Millar, A.H. (2009). Refining the definition of plant mitochondrial presequences through analysis of sorting signals, N-terminal modifications, and cleavage motifs. Plant Physiol. **150:** 1272–1285.

Jänsch, L., Kruft, V., Schmitz, U.K., and Braun, H.P. (1995). Cytochrome c reductase from potato does not comprise three core proteins but contains an additional low-molecular-mass subunit. Eur. J. Biochem. **228:** 878–885.

Laemmli, U.K. (1970). Cleavage of structural proteins during the assembly of the head of bacteriophage T4. Nature **227:** 680–685.

Lazarou, M., Thorburn, D.R., Ryan, M.T., and McKenzie, M. (2009). Assembly of mitochondrial complex I and defects in disease. Biochim. Biophys. Acta **1793:** 78–88.

Leif, H., Sled, V.D., Ohnishi, T., Weiss, H., and Friedrich, T. (1995). Isolation and characterization of the proton-translocating NADH: ubiquinone oxidoreductase from *Escherichia coli*. Eur. J. Biochem. **230:** 538–548.

Leterme, S., and Boutry, M. (1993). Purification and preliminary characterization of mitochondrial complex I (NADH: ubiquinone reductase) from broad bean (*Vicia faba* L.). Plant Physiol. **102:** 435–443.

Martin, V., Villarreal, F., Miras, I., Navaza, A., Haouz, A., González-Lebrero, R.M., Kaufman, S.B., and Zabaleta, E. (2009). Recombinant plant gamma carbonic anhydrase homotrimers bind inorganic carbon. FEBS Lett. **583:** 3425–3430.

May, M.J., and Leaver, C.J. (1993). Oxidative stimulation of glutathione synthesis in *Arabidopsis thaliana* suspension cultures. Plant Physiol. **103:** 621–627.

Meyer, E.H., Taylor, N.L., and Millar, A.H. (2008). Resolving and identifying protein components of plant mitochondrial respiratory complexes using three dimensions of gel electrophoresis. J. Proteome Res. **2:** 786–794.

Millar, A.H., Mittova, V., Kiddle, G., Heazlewood, J.L., Bartoli, C.G., Theodoulou, F.L., and Foyer, C.H. (2003). Control of ascorbate synthesis by respiration and its implications for stress responses. Plant Physiol. **133:** 443–447.

Morgan, D.J., and Sazanov, L.A. (2008). Three-dimensional structure of respiratory complex I from *Escherichia coli* in ice in the presence of nucleotides. Biochim. Biophys. Acta **1777:** 711–718.

Morgner, N., Zickermann, V., Kerscher, S., Wittig, I., Abdrakhmanova, A., Barth, H.D., Brutschy, B., and Brandt, U. (2008). Subunit mass fingerprinting of mitochondrial complex I. Biochim. Biophys. Acta **1777:** 1384–1391.

Neuhoff, V., Arold, N., Taube, D., and Ehrhardt, W. (1988). Improved staining of proteins in polyacrylamide gels including isoelectric focusing gels with clear background at nanogram sensitivity using Coomassie Brilliant Blue G-250 and R-250. Electrophoresis **6:** 255–262.

Peng, G., Fritzsch, G., Zickermann, V., Schägger, H., Mentele, R., Lottspeich, F., Bostina, M., Radermacher, M., Huber, R., Stetter, K.O., and Michel, H. (2003). Isolation, characterization and electron microscopic single particle analysis of the NADH:ubiquinone oxidoreductase (complex I) from the hyperthermophilic eubacterium *Aquifex aeolicus*. Biochemistry **42:** 3032–3039.

Perales, M., Eubel, H., Heinemeyer, J., Colaneri, A., Zabaleta, E., and Braun, H.P. (2005). Disruption of a nuclear gene encoding a mitochondrial gamma carbonic anhydrase reduces complex I and supercomplex I+III_2 levels and alters mitochondrial physiology in Arabidopsis. J. Mol. Biol. **350:** 263–277.

Perales, M., Parisi, G., Fornasari, M.S., Colaneri, A., Villarreal, F., Gonzalez-Schain, N., Echave, J., Gomez-Casati, D., Braun, H.P., Araya, A., and Zabaleta, E. (2004). Gamma carbonic anhydrase like complex interact with plant mitochondrial complex I. Plant Mol. Biol. **56:** 947–995.

Peters, K., Dukina, N.V., Jänsch, L., Braun, H.P., and Boekema, E.J. (2008). A structural investigation of complex I and I+III_2 supercomplex from *Zea mays* at 11–13 Å resolution: Assignment of the carbonic anhydrase domain and evidence for structural heterogeneity within complex I. Biochim. Biophys. Acta **1777:** 84–93.

Pineau, B., Layoune, O., Danon, A., and De Paepe, R. (2008). L-galactono-1,4-lactone dehydrogenase is required for the accumulation of plant respiratory complex I. J. Biol. Chem. **283:** 32500–32505.

Radermacher, M., Ruiz, T., Clason, T., Benjamin, S., Brandt, U., and Zickermann, V. (2006). The three-dimensional structure of complex I from *Yarrowia lipolytica*: A highly dynamic enzyme. J. Struct. Biol. **154:** 269–279.

Rasmusson, A.G., Geisler, D.A., and Møller, I.M. (2008). The multiplicity of dehydrogenases in the electron transport chain of plant mitochondria. Mitochondrion **8:** 47–60.

Rasmusson, A.G., Mendel-Hartvig, J., Møller, I.M., and Wiskich, J.T. (1994). Isolation of the rotenone-sensitive NADH-ubiquinone reductase (Complex I) from red beet mitochondria. Physiol. Plant. **90:** 607–615.

Remacle, C., Barbieri, M.R., Cardol, P., and Hamel, P.P. (2008). Eukaryotic complex I: Functional diversity and experimental systems to unravel the assembly process. Mol. Genet. Genomics **280:** 93–110.

Sazanov, L.A. (2007). Respiratory complex I: Mechanistic and structural insights provided by the crystal structure of the hydrophilic domain. Biochemistry **46:** 2275–2288.

Sazanov, L.A., and Hinchliffe, P. (2006). Structure of the hydrophilic domain of respiratory complex I from *Thermus thermophilus*. Science **311:** 1430–1436.

Sazanov, L.A., Peak-Chew, S.Y., Fearnley, I.M., and Walker, J.E. (2000). Resolution of the membrane domain of bovine complex I into subcomplexes: Implications for the structural organization of the enzyme. Biochemistry **39:** 7229–7235.

Schägger, H., and von Jagow, G. (1987). Tricine-sodium dodecyl sulfate-polyacrylamide gel electrophoresis for the separation of proteins in the range from 1 to 100 kDa. Anal. Biochem. **166:** 368–379.

Sunderhaus, S., Dudkina, N., Jänsch, L., Klodmann, J., Heinemeyer, J., Perales, M., Zabaleta, E., Boekema, E., and Braun, H.P. (2006). Carbonic anhydrase subunits form a matrix-exposed domain attached to the membrane arm of mitochondrial complex I in plants. J. Biol. Chem. **281:** 6482–6488.

Thornber, J.P. (1986). Biochemical characterization and structure of pigment-proteins of photosynthetic organisms. In Encyclopedia of Plant Physiology 19 (New Series), L.A. Stachelin and J.C.J. Arnetzen, eds (Berlin: Springer Verlag), pp. 95–142.

Trost, P., Bonora, P., Scagliarini, S., and Pupillo, P. (1995). Purification and properties of NAD(P)H: (quinone-acceptor) oxidoreductase of sugarbeet cells. Eur. J. Biochem. **234:** 452–458.

Vogel, R.O., Smeitink, J.A., and Nijtmans, L.G. (2007). Human mitochondrial complex I assembly: A dynamic and versatile process. Biochim. Biophys. Acta **1767:** 1215–1227.

Weiss, H., and Juchs, B. (1978). Isolation of a multiprotein complex containing cytochrome b and c_1 from *Neurospora crassa* mitochondria by affinity chromatography on immobilized cytochrome c. Difference in the binding between ferricytochrome c and ferrocytochrome c to the multiprotein complex. Eur. J. Biochem. **88:** 17–28.

Werhahn, W.H., Niemeyer, A., Jänsch, L., Kruft, V., Schmitz, U.K., and Braun, H.P. (2001). Purification and characterization of the preprotein translocase of the outer mitochondrial membrane from *Arabidopsis thaliana*: Identification of multiple forms of TOM20. Plant Physiol. **125:** 943–954.

Wittig, I., Braun, H.P., and Schägger, H. (2006). Blue-native PAGE. Nat. Protoc. **1:** 418–428.

Zerbetto, E., Vergani, L., and Dabbeni-Sala, F. (1997). Quantification of muscle mitochondrial oxidative phosphorylation enzymes via histochemical staining of blue native polyacrylamide gels. Electrophoresis **18:** 2059–2064.

Zickermann, V., Dröse, S., Tocilescu, M.A., Zwicker, K., Kerscher, S., and Brandt, U. (2008). Challenges in elucidating structure and mechanism of proton pumping NADH:ubiquinone oxidoreductase (complex I). J. Bioenerg. Biomembr. **40:** 475–483.

Zickermann, V., Kerscher, S., Zwicker, K., Tocilescu, M.A., Radermacher, M., and Brandt, U. (2009). Architecture of complex I and its implications for electron transfer and proton pumping. Biochim. Biophys. Acta **1787:** 574–583.